Calcium and zinc differentially affect the structure of lipid membranes

Norbert Kučerka, [* a,b] *Ermuhammad Dushanov,* [c] *Kholmirzo T. Kholmurodov,* [b,d] *John Katsaras,* [e-g] *and Daniela Uhríková* [a]

[a] Department of Physical Chemistry of Drugs, Faculty of Pharmacy, Comenius University in Bratislava, 83232 Bratislava, Slovakia

[b] Frank Laboratory of Neutron Physics, [c] Laboratory of Radiation Biology, Joint Institute for Nuclear Research, 141980 Dubna - Moscow Region, Russia

[d] Dubna State University, 141980 Dubna - Moscow region, Russia

[e] Shull Wollan Center, a Joint Institute for Neutron Sciences, [f] Biology and Soft Matter Division, Oak Ridge National Laboratory, Oak Ridge, Tennessee 37831

[g] Department of Physics and Astronomy, University of Tennessee, Knoxville, Tennessee 37996, United States

1

ABSTRACT

Interactions of calcium (Ca^{2+}) and zinc (Zn^{2+}) cations with biomimetic membranes made of dipalmitoyl-phosphatidylcholine (DPPC) were studied by small angle neutron diffraction (SAND). Experiments show that the structure of these lipid bilayers is differentially affected by the two divalent cations. Initially, both Ca^{2+} and Zn^{2+} cause DPPC bilayers to thicken, while further increases in Ca^{2+} concentration result in the bilayer thinning, – eventually reverting to having the same thickness as pure DPPC. The binding of Zn^{2+}, on the other hand, causes the bilayers to swell to a maximum thickness, and the addition of more Zn^{2+} does not result in a further thickening of the membrane. Agreement between our results obtained using oriented planar membranes and those from vesicular samples implies that the effect of cations on bilayer thickness is the result of electrostatic interactions, rather than geometrical constraints due to bilayer curvature. This notion is further reinforced by MD simulations. Finally, the radial distribution functions reveal a strong interaction between Ca^{2+} and the phosphate oxygens, while Zn^{2+} shows a much weaker binding specificity.

INTRODUCTION

Plasma membrane properties such as membrane fluidity, bending and compressibility moduli, electrostatics, and aggregation and fusion are associated with ions that are present in the cytosol and the extracellular fluid. Not surprisingly, divalent metal cations have been found to play a prominent role with regards to bilayer structure.[1] Metals such as calcium, magnesium, iron, manganese, copper, zinc, nickel and cobalt, although known to be toxic beyond a certain concentration, are essential to life. Among the large group of divalent metal cations, calcium and zinc attract a special interest due to their peculiar properties.

Calcium belongs to the alkaline earth metals and plays an important role in many cellular processes.[2-4] It has been shown to contribute to specific interactions within bacterial membranes that ~~resulted in the~~ limit~~ation of~~ water penetration, to mention but one example.[5] Zinc, amid the first-row of transition metals, is also ~~found likewise~~ attractive to study as it is second only to iron in terms of abundance and importance in biological systems.[6] Zn^{2+} is known to play a fundamental role in several critical cellular functions such as protein metabolism, gene expression, the structural and functional integrity of biomembranes, and in metabolic processes.[7,8] Although a complete understanding of the physicochemical processes taking place in biomembranes has yet to be established, their functionality is known to depend strongly on the type of ion, the chemical composition of the membrane's interface, its thermodynamical state, and degree of hydration. For example, both Zn^{2+} and Ca^{2+} have been found to deviate from an inversely linear correlation between the ion's ionic radius and its effect on shifting the lipid phase transition temperature.[1] What makes these cations different from others, and from each other, remains an open question.

In spite of the importance of divalent cations in biological membranes, their adsorption to phosphatidylcholine membranes and their influence on lipid bilayers is far from being understood.[9,10] While dehydrated planar stacks of multibilayers swelled upon the addition of different cations without any apparent structural changes to bilayers themselves[11] — similarly to the results of high monovalent salt concentration studies[12,13] suggesting ~~however~~ the possibility of phase separation[14] — a more complex behavior was displayed by fully hydrated, curved bilayers in the presence of Ca^{2+}.[10,15,16] Effects due to curvature, nevertheless, may be entangled with those due to electrostatic interactions, as has been suggested recently.[17]

It is important to decouple effects due to electrostatic interactions from those imposed by geometrical constraints found in curved vesicular bilayers, in order to associate the mode of

interaction of the individual cations with the lipid membranes. Small-angle neutron-diffraction (SAND) experiments were designed to utilize planar bilayers, extending previous studies on the effects of calcium and zinc on biomimetic membranes of dipalmitoyl-phosphatidylcholine (DPPC). SAND allows for the in situ manipulation of sample conditions, but more importantly, provides quantitative data on the distribution of structural moieties, their sizes, shapes and correlation lengths.[18] Variations in diffraction maxima can signal important changes to membrane structure, which in turn, may have biological implications. Our current observations agree well with the notion that ions affect the interface of membranes, results that can most likely be rationalized in terms of electrostatic interactions, rather than geometrical constraints due to bilayer curvature. Our results then highlight the importance of these cations with regards to membrane structure, and possibly function.

The refinement of the structural changes measured experimentally on the molecular scale was also performed on the atomistic level using results from molecular dynamics (MD) simulations. Although MD simulations offer structural resolution not attainable by experiment, prudence must nonetheless be exercised.[13,19,20] Based on a combination of experimentally obtained SAND data and MD simulations, we are able to observe structural changes in lipid bilayers due to interactions with Ca^{2+} and Zn^{2+} cations, and assign differences between the cations to differences in the specificity of their interactions with the membrane.

MATERIALS AND METHODS

Sample preparation

1,2-Dipalmitoyl-*sn*-glycero-3-phosphocholine (DPPC) was purchased from Avanti Polar Lipids (Alabaster, AL) and used without further purification. $CaCl_2$ and $ZnCl_2$ salts, and organic solvents were obtained from Fisher Scientific Company (Ontario). Approximately 15 mg of lipid

(thin film comprising of ~2,500 bilayers ~~with~~ having a total thickness ~15 μm when spread onto a 25 x 60 mm^2 silicon wafer) was co-solubilized with appropriate amounts of salt in a 1:1 (vol/vol) solution of chloroform:trifluoroethanol, or in deionized water (18.3 MΩ cm), and mixed thoroughly using a vortex mixer, or several freeze-thaw cycles in the case of the water solution samples. The dispersions prepared in organic solvent were deposited onto silicon wafers and rocked during evaporation in a glove box to form highly oriented multilayer stacks, while the remaining traces of solvent ~~traces~~ were removed by placing the samples under vacuum.[21] High quality oriented stacks were confirmed by observing 7-9 orders of diffraction peaks, and the narrow width of the central peak in the rocking curves shown in e.g., Fig. 1 and Figs. S1-S3.
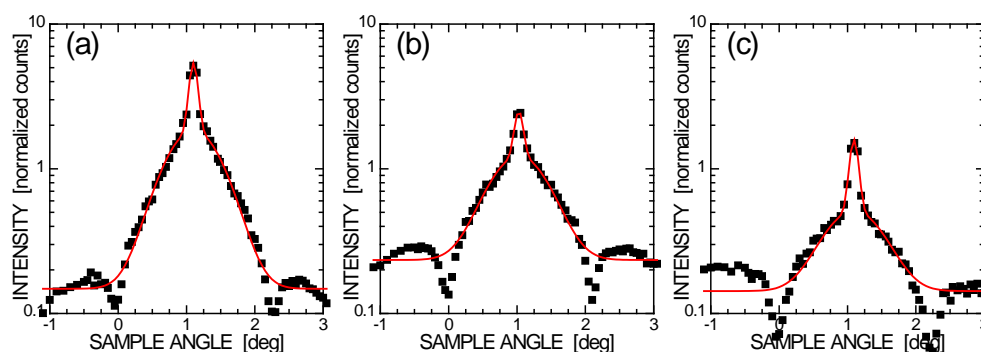
Figure 1. Uncorrected rocking curves (i.e., normalized intensities measured as a function of sample angle) from aligned (a) DPPC multibilayers, and DPPC mixed with Ca^{2+} at 1:0.2 molar ratio in (b) solvent or (c) water solution. Data were collected with the detector located at the position of the first Bragg diffraction. The sample mosaicity, estimated from the Gaussian fit to the central narrow peak, is ~0.06 degree for all three samples. Note that two minima are the result of increased neutron absorption, which occurs when the sample is rotated so that either the incident beam or the diffracted beam is parallel to the substrate. These "wings" were not corrected as was done elsewhere.[22]

Rocking curves for samples with increasing concentration of cations (shown in Fig. S2 of the supporting information) revealed an ever-decreasing degree of sample alignment. This was more pronounced in the case of Zn^{2+} ions, where a visual inspection suggested samples having macroscopic domains of crystalized ions. These samples were excluded from further measurements. The situation was ameliorated by modifying the sample preparation procedure, where DPPC and salt were co-solubilized in water, as opposed to organic solvent. The Zn^{2+} containing bilayers mixed in water solution were deposited on a silicon wafer that was heated to $50^{o}C$, until the excess water evaporated. For both sample preparation protocols, care was taken to form lipid multilayers in the fluid phase, and to anneal the samples for several hours upon the rehydration.

Comparing the rocking curves of samples prepared through the deposition from solvent and water solution (Fig. 1b and 1c) confirms that the two samples are of comparable quality in the case of DPPC+Ca^{2+} (1:0.2 mol/mol), while a significant improvement was achieved in the case of the Zn^{2+} loaded samples. All the Zn^{2+} containing bilayers were then deposited from water solution. All samples considered in our study had rocking curves with mosaicity of less than 0.1 degree, as shown for the selected samples in figures S1-S3.

Small-Angle Neutron Diffraction

Neutron diffraction data were collected at the Canadian Neutron Beam Centre's (CNBC) N5 beamline located at the National Research Universal (NRU) reactor (Chalk River, Ontario, Canada). 2.37 Å wavelength neutrons were selected by the (002) reflection of a pyrolytic graphite (PG) monochromator, and a PG filter was used to eliminate its higher order reflections. Despite reducing the intensity of the higher harmonics (i.e., $\lambda/2$, $\lambda/3$, $\lambda/4$ etc.) down to ~1%, diffraction peaks from the silicon monocrystal wafers had to be discarded on a case-by-case

6

basis. Si peaks were identified by the fact that they remained stationary as a function of temperature or changes in hydration, while peaks due to the membrane shifted in angle (see Fig. S7-S9 in the Supporting Information).

Incident neutrons were collimated (6x50 mm^2 collimator). At the sample, the neutron beam was ~8 mm wide (FWHM) with a horizontal angular divergence of 26'. A set of 7x40mm^2 slits — before and after the sample — were utilized to place the neutron beam at the sample center of the sample. Neutrons diffracted by the sample, and collimated by another rectangular collimator of 4x50 mm^2 opening with a horizontal angular divergence of ~17' were then collected by a multi-wire ^{3}He detector. We define the sample and detector angles as Ψ and Φ, respectively.

Diffraction data were collected following the standard symmetric diffraction scans, in which reciprocal space was probed along the z direction of the scattering vector Q. This was achieved by rotating the sample angle by half the detector angle ($\Phi=2\Psi$), resulting in the in-plane Q component being zero. The Q_{in} component was obtained in separate measurements following the mode used for collecting rocking curve data. In this mode, the detector is positioned at the first Bragg reflection and the sample is scanned through a number of angles enabling one to interrogate reciprocal space along constant $|Q|$ values (i.e., $Q_z^2 + Q_{in}^2 = Q^2$). The diffraction curve mode is used to obtain the one-dimensional neutron scattering length density (NSLD) profile, while rocking curves across the diffraction peak allow for the evaluation of sample quality, independent of the peak position.[23] Note, that measured intensities need to be corrected for incident flux, sample absorption, and the Lorentz correction according to well-established procedures for obtaining proper NSLD profiles.[22,24] However, this is not necessary in the case of rocking curves, where the evaluated parameter is only the peak width.

Samples were held vertically in an air-tight hydration chamber at 25°C. The chamber's bottom was filled with a saturated K_2SO_4 (97% RH)[25] solution of different D_2O/H_2O mixtures. The well-controlled hydration conditions, which were slightly below the full hydration condition, restrict bilayer undulations important for determining bilayer material properties,[26] but assure that the sample is stable throughout the course of the experiment. Under these conditions, the amount of inter-bilayer hydration water is sufficient to avoid structural changes due to steric constraints.[24]

Molecular Dynamics Simulations

Molecular Dynamics simulations using GROMACS 5.0.4[27] package were performed using 128 DPPC and 3655 water molecules. 18 water molecules were replaced by cations in Me^{2+} loaded bilayers (additional 36 water molecules were replaced by Cl^- counter ions) to achieve a DPPC:Me^{2+} ratio of 1:0.14 mol/mol, while 64 Me^{2+} cations (and 128 Cl^-) were needed for the ratio 1:0.5 mol/mol ratio. The initial topology was taken from literature.[28] Modeling was carried out in three stages: i) minimization of the energy; ii) NVT and NPT equilibration of the system; and iii) molecular dynamics (MD) calculations with the GROMOS96_53A6 force field and parameters of expansion taken from Berger lipids.[29] Simulation convergence was assessed using the area per lipid parameter, which suggested an equilibration time of about 30ns (see Fig. S11). The production run continued for an additional 50ns.

GridMAT-MD[30] was used to calculate the average deviation of lipid membrane thickness (D_M) and area per lipid (A_L), while radial distribution functions were calculated using the GROMACS auxiliary program. SIMtoEXP[19] was used to verify the simulated results with those obtained from neutron diffraction experiments (see Fig. S12-S14).

RESULTS AND DISCUSSION

We screened multiple copies of samples using the above described rocking curve measurements. The best quality samples exhibited narrow central peaks and up to 7-9 orders of quasi-Bragg maxima (Fig. 2, Fig. S4-S6, S10). All diffraction experiments involved contrast variation measurements, in which different D_2O/H_2O ratio solutions were utilized to hydrate the samples. This approach allowed us to solve the scattering phase problem for our centro-symmetric system by requiring the scattering form factors to change linearly as a function of D_2O content.[31] We also employed the procedure suggested for unambiguous phase determination as described in details elsewhere.[24]
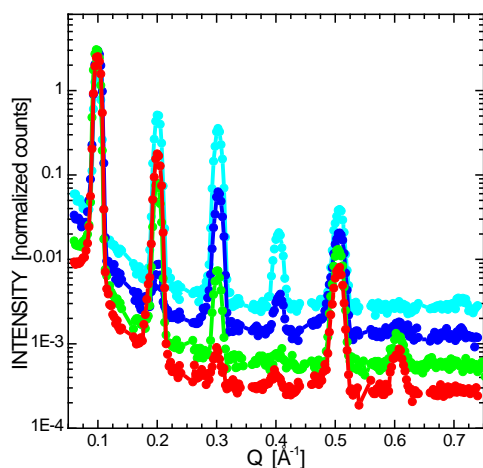
Figure 2. Uncorrected diffraction curves (i.e., normalized intensities measured as a function of scattering vector) from aligned DPPC multibilayers containing Zn^{2+} (DPPC:Zn^{2+}=1:0.096 mol/mol), and measured in 100% (red), 70% (green), 40% (blue), and 8% (cyan) D_2O contrast conditions. The curves were shifted vertically for clarity of viewing.

The one-dimensional NSLD bilayer profiles were obtained by Fourier transformation of the corrected contrast varied diffraction data.[24] While the profile corresponding to the 100% D_2O

contrast condition provides the best estimate of the bilayer's steric thickness, lower contrast profiles reveal details ~~in the region~~ of the lipid head-group region. This is best exemplified by the 8% D_2O data, where the net NSLD of water is zero, essentially yielding the lipid only NSLD profile of the bilayer (Fig. 3a). In addition, the contrast varied diffraction data can be subtracted from each other either in real space (e.g., NSLD profiles from Fig. 3a) or in reciprocal space (e.g., structure factors obtained from Fig. 2), resulting in the probability distributions of water and lipid molecules.[24]
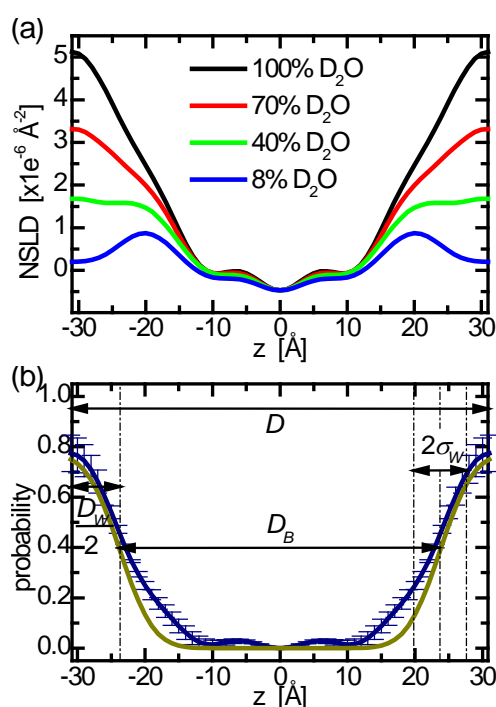
Figure 3. (a) DPPC bilayers prepared with Zn^{2+} (DPPC:Zn^{2+}=1:0.096 mol/mol) shown through the one-dimensional NSLD profiles calculated from SAND measurements at different contrast conditions. (b) The water probability distribution obtained using the NSLD subtraction procedure (blue line), and by fitting the error function to the contrast varied diffraction data (green line).

The multilayer repeat distance D is the sum of the bilayer thickness D_B and interbilayer water space D_W. σ_W, defined by the width of error function, determines the roughness of water-bilayer interface.

Figure 3b shows water probability distributions obtained from ~~by~~ subtractions in real and reciprocal space. The former approach does not require any assumptions on the functional form of the NSLD profile, nor of the probability distribution resulting from a direct subtraction. The water distribution is obtained from averaging all of the separately subtracted pairs of contrast varied NSLD profiles, which also provides an estimate of the standard deviation error (blue line in Fig. 3b). On the other hand, the advantage of the latter approach lies in the simultaneous evaluation of all the different contrast variation diffraction data, while assuming that the water probability follows an error function, as described previously.[24] We adopted this approach for the data analysis used to obtain the inter-bilayer water layer thickness D_W, roughness of water-bilayer interface σ_W, and bilayer thickness D_B from the resulting error function ~~directly~~ (see Fig. 3b for the graphics of $D=D_B+D_W$ definition).

The above-obtained parameters allow us to calculate the area per unit cell A_{UC} from the known DPPC molecular volume V_L (1147 Å^3),[32] and volumes estimated for Ca^{2+} (20.1 Å^3) and Zn^{2+} (12.5 Å^3) ions.[33] A_{UC} is an important value of the lateral forces taking place within lipid bilayers, and also allows us to place the data on an absolute scale. The form factor F_0 corresponding to the forward scattering that is not available from the scattering experiment, is calculated in a manner similar to what was done previously for X-ray scattering[34]

$$F_0^{abs} = \left(b_{UC} - \rho_W V_{UC} \right) / A_{UC} \,. \tag{1}$$

Here, b_{UC} represents the neutron scattering length[35] of the unit cell moieties whose volume V_{UC} displaces an equivalent volume of water molecules, with a neutron scattering length density ρ_w. All parameters in the brackets are well known, while A_{UC} is determined from the probability distributions discussed above. The calculation then consists of several iterations, converging on the final structural and normalization parameters.

It is worth noting that the calculated ~~water~~ probability distributions ~~of water~~ (see Fig. 3b) can assume values from 0 to less than 1. This suggests that the two component system consists of a region occupied completely by lipid (z=-15 to 15 approximately) and a ~~region of~~ lipid/water mixture ~~region~~ (be~~l~~low z=-15 and above z=15). Interestingly, the water probability levels out before reaching a value of 1, suggesting that the system does not contain a pure water layer. It is also interesting to note a systematic difference between the reciprocal space and real space analyses, which varies by up to 2 Å. While the first method averages over the four different contrast conditions in reciprocal space, the second method treats the diffraction data obtained at different contrast conditions individually, and then averages the results in real space. More important, however, is that the two methods show excellent agreement when it comes to relative structural changes.[24] Table 1 and 2 list the parameters evaluated according to the second method.

Table 1. Parameters calculated for DPPC multilayers with Ca^{2+} ions at 25°C and 97%RH.

| DPPC:Ca^{2+} [mol/mol]	D [Å]	D_W [Å]	σ_W [Å]	D_B [Å]	A_{UC} [Å^2]
1:0	60.3	13.6	4.0	46.7	49.1
1:0.100	63.5	15.6	3.9	47.8	48.0
1:0.125	63.9	15.3	4.3	48.6	47.3
1:0.143	63.5	12.5	3.0	51.0	45.0
1:0.200	63.5	13.0	3.9	50.5	45.5
1:0.300	64.0	15.6	4.7	48.4	47.6
1:0.400	63.9	16.6	4.0	47.4	48.8
1:0.500	64.4	17.0	4.2	47.4	48.9

Table 2. Parameters calculated for DPPC multilayers with Zn^{2+} ions at 25°C and 97%RH.

DPPC:Zn^{2+} [mol/mol]	D [Å]	D_W [Å]	σ_W [Å]	D_B [Å]	A_{UC} [Å^2]
1:0	60.3	13.6	4.0	46.7	49.1
1:0.032	60.6	14.1	4.5	46.5	49.4
1:0.096	61.6	14.2	3.9	47.4	48.5
1:0.100	62.5	13.1	4.5	49.4	46.5
1:0.125	62.5	13.5	5.0	49.0	46.8
1:0.143	63.3	13.8	4.2	49.5	46.4
1:0.160	62.5	14.1	4.1	48.4	47.6
1:0.200	63.8	14.4	3.9	49.4	46.6
1:0.240	62.8	13.8	3.3	49.0	47.1
1:0.333	64.6	15.4	4.1	49.2	46.8
1:0.500	64.5	15.2	3.9	49.3	46.8

The ~~obtained~~ results confirm that both cations bind to DPPC bilayers. This fact is reflected in the increased lamellar repeat distance D that is most likely the result of charge induced repulsion between bilayers. This observation is consistent with previously published results, in which zwitterionic lipid multilayers swelled in the presence of different types of salts.[11,12,15,36] For example, $CaCl_2$ at 1-50 millimolar concentrations induced fluid multibilayers to swell to the point that they became unbound (i.e., infinite D)~~, and~~ — not unlike our current observations — and D reached ~~had~~ an upper limit in the gel phase.[15,36] Inoko et al.[37] explained that the initial swelling was due to an increase in inter-bilayer electrostatic repulsion that was screened at high salt concentrations. Supposedly membrane structure was not affected at high salt concentrations.[12] Interestingly, our low salt concentration results reveal that both D_B and D_W contribute to the increases in D. Moreover, Ca^{2+} and Zn^{2+} do not have the same effect on D.

Fig. 4a shows a monotonic increase of D and D_B up to a Zn^{2+}:DPPC ratio of 0.14 mol/mol, after which they both seem to plateau, with ~~the bilayer thickness~~ D_B experiencing almost twice

the change of D_W (see Table 2). Calculated area per unit cell that comprises of a DPPC molecule and the appropriate amount of cations follows the thickness changes, decreasing with an increasing Zn^{2+}:DPPC ratio. This is due to the fact that lateral area and transverse thickness are inversely related (i.e., $A_{UC}=V_{UC}/D_B$).
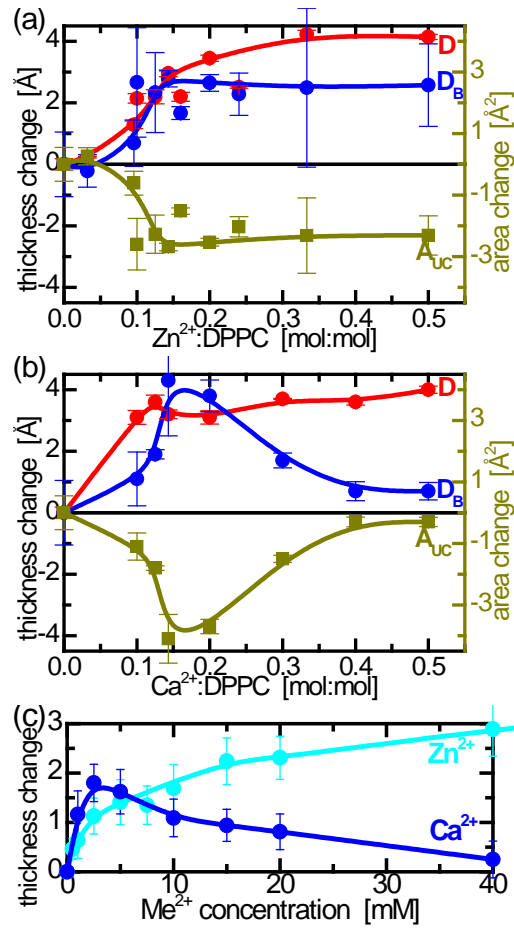
Figure 4. (a) Zn^{2+} and (b) Ca^{2+} cation-induced changes to bilayer structure expressed through the lamellar repeat distance D (red), bilayer thickness D_B (blue), and area per unit cell A_{UC} (dark yellow). (c) Previously published results of cation-induced changes to the bilayer structure of unilamellar vesicles dispersed in water solution.[10,16] Changes are calculated with respect to neat

14

DPPC bilayers, and uncertainties are estimated from the partial derivatives of the chi-square function.

Bilayers with Ca^{2+} behave differently from those with Zn^{2+}. While they both experience similar changes for ion:DPPC ratios up to 0.14 mol/mol, they differ at higher ratios. The most pronounced difference is exhibited by D_B, which experiences a decrease at high concentrations of Ca^{2+}, ~~displaying~~ with a maximum at DPPC:Ca^{2+}=1:0.14 mol/mol. D_B decreases almost to the level of pure DPPC bilayers at high Ca^{2+}:DPPC ~~the high~~ ratios, while the changes are compensated by the changes in D_W, resulting in a D that is practically unaffected by changes in Ca^{2+} concentration. We can therefore disregard the effect that adjacent bilayers have on each other in our stacked system. This is supported by our previously published results[10,16] (reproduced in Fig. 4c), whereby unilamellar vesicles dispersed in the water solution loaded with either Zn^{2+} or Ca^{2+} ions displayed trends similar to those in our present data. The data also imply that a small curvature present in the unilamellar vesicles is not an important factor affecting the bilayer structure of ion containing DPPC membranes.

It is interesting to note that recently published studies indicate a behavior of cation-containing lipid bilayers to be different at low and high hydration conditions. Alsop et al. reported that lipid headgroups hydrated by less than 7 water molecules (50% RH) are not affected by the addition of salt cations, and any changes are manifested by an increase of inter-bilayer water layer thickness.[11] Changes to lipid bilayer structure apparently require the presence of a sufficient number of water molecules. The critical number of water molecules for neat POPC bilayers has been suggested to be 3, while in the case of POPC + Ca^{2+} and POPC + Zn^{2+} complexes the critical number is ~7.[1] Our observation of changes to D_B and D_W at 97% RH support the high

15

hydration scenario. These changes — in the form of headgroup-salt complexes — in turn induce changes to the ordering of the lipid hydrocarbon chains, as noted previously.[15]

We used MD simulations to determine the atomistic structural details of the most interesting concentration of cations, namely the 1:0.14 molar ratio of DPPC:Me^{2+}. Simulation results were first validated by the experimentally obtained diffraction data using the simulation-to-experiment (SIMtoEXP) approach.[19] The SIMtoEXP procedure calculates scattering form factors from simulations without model assumptions using a Fourier Transform and comparing them directly to experiment. Doing this reveals local deviations. Differences between experiment and simulations are not unexpected due to the less than perfect force fields used,[20] and the small differences in hydration levels. Simulations give rise to smoother profiles, while those from experiment contain more features (compare e.g., Fig. 3a and S12-S14). Simulations, however, are capable of deconstructing the bilayer into smaller structural subunits that allow the determination of important structural information. Figure 5 focuses on the head-group's phosphate and carbonyl groups, which are anticipated to be the primary targets for cations binding due to their charges.
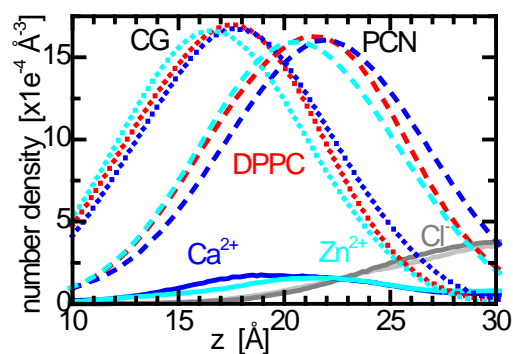
Figure 5. Simulated number density distributions along the bilayer normal (bilayer is centered at z=0 Å) focusing on the carbonyl-glycerol (CG - dotted lines) and phosphate-choline groups

(PCN - dashed lines) for a pure DPPC bilayer (red), and bilayers containing Ca^{2+} (blue) or Zn^{2+} (cyan) cations. Note the nearly identical distributions of Cl^- counter ions (gray), mostly outside the bilayer, for both salts.

The addition of $CaCl_2$ or $ZnCl_2$ salt affects gel phase DPPC bilayers, as is evident by the positional changes within their headgroup regions. The effect of Cl^- anions is ~~can be~~ ~~negle~~negligible, ~~cted,~~ based on the fact that their influence is ~~they reside~~ mostly outside the bilayer. This is in agreement with the observation of weak interactions between various anions and the lipid liquid-condensed phase.[38] The ~~distinct~~ effects as a result of ~~of~~ cations are~~is~~, however, expected based on their ~~different~~ location~~s~~. While Ca^{2+} causes both the carbonyl and phosphate groups to shift slightly outwards, the shifting effect of Zn^{2+} is towards the bilayer center. Moreover, the cations themselves seem to be localized in opposite directions. Ca^{2+} penetrates deeper into the lipid bilayer, positioning itself about 1.5Å below the maximum of the phosphate distribution, while Zn^{2+} is positioned about 1.5Å above the phosphate maximum. Nevertheless, in both cases the distribution functions in Fig. 5 suggest the primary binding site for both cations to be the phosphate group, in contrast to what was observed in dehydrated bilayers.[11]

We further analyzed our simulation data in order to characterize the extent of the specific binding of the two cations. As confirmed by the radial distribution functions (RDF) calculated from our simulations, both cations interact strongly with the negatively charged oxygens. Previous simulation results suggested carbonyl oxygens to be their main target,[39] although other studies questioned the reliability of the force-fields utilized in the different simulations.[13] Our data (left hand graphs of Figure 6) clearly show that both Ca^{2+} and Zn^{2+} (at DPPC:Me^{2+}=1:0.143 mol/mol) interact with carbonyl oxygens only a third as much as they interact with the phosphate

17

oxygens (O16 and O35 curves vs. O9 and O10 in Fig. 6 – see Fig. S15 for <u>the</u> ~~the schematics of~~

naming convention <u>used</u>). The graphs also show that Ca^{2+} forms a contact pair with phosphate

oxygens (blue and magenta curves in Fig. 6a) that is about two times stronger than that formed

by Zn^{2+} (blue and magenta curves in Fig. 6b). A similar ratio is also observed in the case of the

RDF calculated for carbonyl oxygen (dark yellow curves in Fig. 6). In addition to confirming the

preferential interactions of both cations with phosphate, the data show that Ca^{2+} binds with the

phosphate group much more readily than Zn^{2+} at <u>a</u> ~~the~~ DPPC:Me^{2+} molar ratio of 1:0.143. In

fact, without exception Ca^{2+} binds to any head-group atom much more favorably than Zn^{2+}.
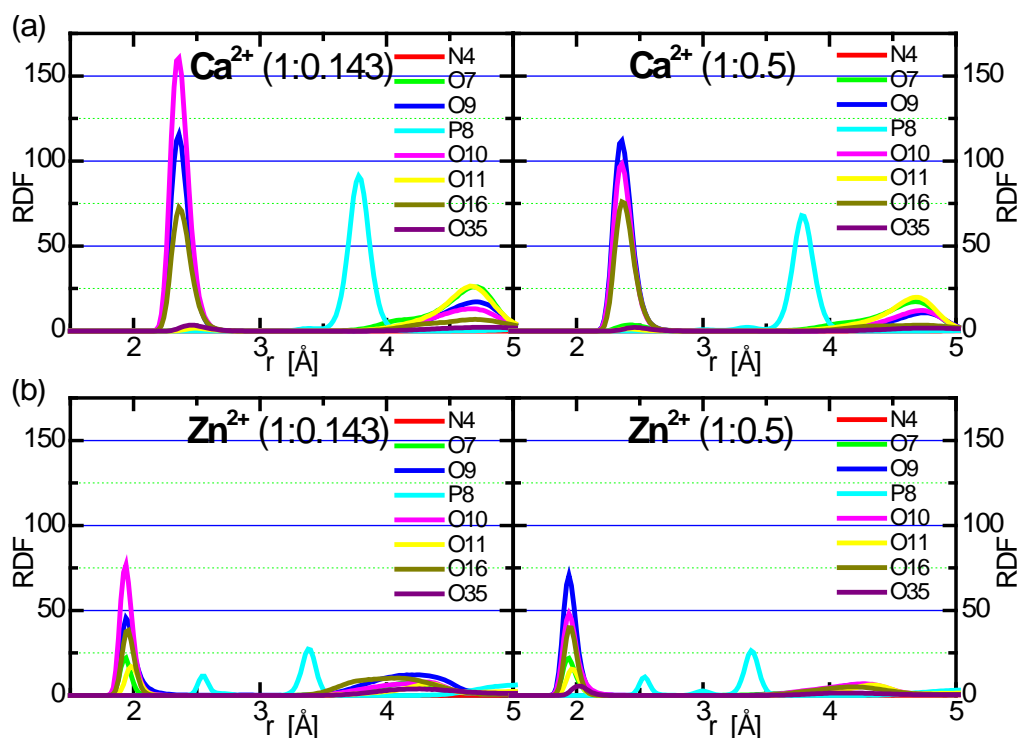
Figure 6: Radial distribution functions (RDF) for (a) Ca^{2+}- and (b) Zn^{2+}-lipid headgroup atom
pairs from simulations performed at ion:DPPC ratios of 0.143 (left-hand) and 0.5 (right-hand).

The RDF is shown for different headgroup atoms, starting from ~~in the order from~~ the bilayer exterior, inwards.

Interestingly, the ~~The~~ situation changed ~~intriguingly~~ when a~~n~~ Me^{2+}:DPPC ratio of 0.5 mol/mol was used in our simulation – the ratio at which experimental results revealed differences in the effects between the two cations. Firstly, the specific binding with the phosphate O10 oxygen decreases markedly for both cations (see the right-hand graphs of Figure 6). However, this decrease is, for the most part, offset by an increased binding of Zn^{2+} with O9 oxygen. In the case of Ca^{2+} there is an overall decrease of phosphate group specific binding for Ca^{2+} by about 20%, despite a 3.5-fold increase in ion concentration. This decrease in specific binding then explains the decreased effect that Ca^{2+} cations have on the experimentally observed bilayer thickness and area per lipid ~~observed experimentally~~. The strong, initial effect on the lipid headgroup by Ca^{2+}, which also affects the hydrocarbon chain region, is likely screened at higher cation concentrations.[15] Moreover, the constant level of Zn^{2+} specific binding agrees well with what we saw experimentally regarding DPPC bilayer structure.

The differences between the structural changes experienced by DPPC bilayers when Ca^{2+} or Zn^{2+} are introduced may also be rationalized by the physical differences between the two cations.[1] Calcium ions have a larger ionic, or Pauling radius (1 Å), than zinc ions (0.75 Å). The preferred coordination number for bulk hydrated calcium has been reported to be between 6 and 8,[1] while for zinc ~~ions~~ this number is between 4 and 6.[7] In addition, the hydrogen bonding of water molecules extends beyond the ion's primary hydration shell — their crystal arrangements in bulk water have been proposed to be $Zn[H_2O]_6^{2+} \bullet [H_2O]_{12}$ [40] and $Ca[H_2O]_{6.1}^{2+} \bullet [H_2O]_{5.29}$.[41]

Calcium ions as a consequence of their larger size, require smaller amounts of energy for the removal of hydration shell water.[42]

Up to this point we have discussed experimental and simulation data ~~It is in order to have a closer look at interactions~~ of ion-containing lipids ~~and ions~~ with water ~~— one of the tiniest and often forgotten biomolecules~~.[43] ~~The most of the data discussed above have been obtained utilizing various experimental methods.~~ Theoretical approaches, however, ~~on the other hand,~~ can provide additional information regarding ~~in~~ both the structure and dynamics of ion hydration. The hydration energies that are routinely calculated ~~regularly~~ are unfortunately often poor or require the input of unrealistic ion characteristics,[41] ~~–~~ although ~~the~~ there are recent MD simulations that are in good ~~provide quantitative~~ agreement with experimental data.[39] The difficulties lie in the fact that water molecules surrounding ~~the~~ ions are strongly polarized, something not well addressed by ~~that is in turn a weak spot of~~ MD force fields.[44] In addition, the water binding capacity of ions is ~~nevertheless distinctly~~ reduced in the case of ion-lipid complex formation, suggesting that both ion and lipid ~~sacrifice~~ give up to 50% of their hydration shell.[6] Ions have been found to disrupt water structure, reducing its ability to solvate lipid head-groups, and ~~whereas~~ a monotonic dependence on the size of monovalent cations has ~~ave~~ been reported.[45] According to our MD simulation results, divalent Ca^{2+} ions create about 1.6 times fewer pairs with surrounding water molecules than do Zn^{2+} ions (Fig. 7) when interacting with DPPC bilayers. This smaller ~~lesser~~ Ca^{2+} hydration shell most likely allows for ~~its~~ more proximal ~~closer~~ and stronger contacts with the lipid phosphate.

20
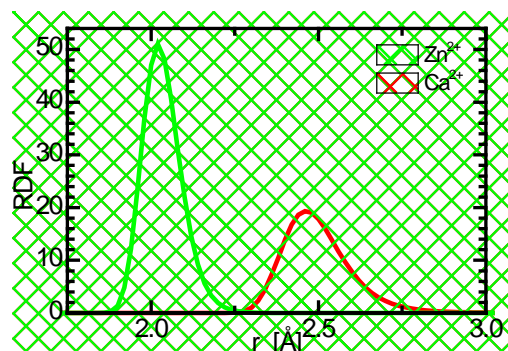
Figure 7: Radial distribution functions (RDF) for Zn^{2+}- and Ca^{2+}-water pairs determined from MD simulations. The peak position provides a mean radius for the of primary hydration shell (larger for Ca^{2+} when compared to Zn^{2+}). The area under the peaks corresponds to the number of water molecules present in the hydration shell of each cation interacting with the lipid bilayer (this value is smaller for Ca^{2+}. when compared to Zn^{2+}).

Our simulation data corroborate that the electronic structure of calcium results for in its high affinity for PO_4, affinity in particular (also partly for CO_2 also).[12] The electronic structure of zinc, on the other hand, differs from that of other divalent metal ions. Calculations have suggested significant variability in the modes of binding of hydrated Zn^{2+}, while their binding energies vary only by small amounts.[46] This can then explain the low specificity of zinc binding to lipid bilayers and the non-specific changes to their structure. In our case, this characteristic may have manifested itself in the monotonic increase of the experimentally determined structural parameters, which are unaffected at higher concentration of the cation. The other divalent metals may, however behave differently. For example, Mg^{2+} and Fe^{2+} are for example known to have ionic size and hydration shells similar to those that of Zn^{2+},[40,47] yet they have been reported to cause even higher repulsion between the lipid bilayers, compared to the than in the case of larger

21

Ca^{2+}.[11] It is clear that ~~Such findings may propose the high specificities of those cations that can likely prevail other structural properties in their overall effect. After all, how to better explain special physiological roles these cations play in the functionality of membrane? The~~ further studies examining the lipid-ion interactions ~~in the case~~ of Mg^{2+}, Fe^{2+} are needed to ~~clearly in order to~~ answer this perplexing ~~intriguing~~ question.

CONCLUSIONS

Using SAND and MD simulations we observed differences in how Ca^{2+} and Zn^{2+} affect DPPC bilayers – i.e., changes in lipid bilayer thickness. For both cations, bilayer thickness increased, reaching a maximum at ~1:0.14 mol/mol DPPC:Me^{2+}. However, while further increases in Ca^{2+} concentration resulted in the bilayer thinning to a level not dissimilar from that of pure DPPC bilayers, Zn^{2+} binding exhibited ~~the~~ behavior of a typical binding isotherm, reaching a level where further addition of the cation resulted in no change to the bilayer. The radial distribution functions of cation-lipid pairs calculated from MD simulations for several lipid head group atoms revealed Ca^{2+} binding strongly to the phosphate group, while Zn^{2+} had ~~s~~ a much lower binding affinity for all head-group atoms. Our results also confirmed that the observed structural changes could be rationalized in terms of electrostatic interactions, rather than ~~of~~ geometrical constraints due to bilayer curvature, thus reinforcing the chemical importance of the two cations. In addition, our observations imply that lipid-ion interactions do not only depend on which cation is present, but also on the lipid's thermodynamic state and its level of hydration. It will be interesting to expand these studies by examining the effect of other cations, and/or the role of lipid structural properties. An understanding of lipid bilayer structural changes as a result of different salt environments provides a foundation for better insights into the structure-function relationships that most certainly take place in more complicated biomembrane systems.

ASSOCIATED CONTENT

~~Complete e~~ Additional experimental and simulation data ~~neutron rocking curves and diffraction data, and graphics of a direct validation of MD simulations by experimental data~~ are included in the ~~as~~ Supporting Information. This material is available free of charge via the Internet at http://pubs.acs.org.

REFERENCES

1. Binder, H.; Zschornig, O. The effect of metal cations on the phase behavior and hydration characteristics of phospholipid membranes. *Chem.Phys Lipids* **2002,** *115*(1-2), 39-61.

2. Lee, A. G.   How lipids affect the activities of integral membrane proteins. *Biochim.Biophys.Acta* **2004,** *1666*(1-2), 62-87.

3. Lee, H. C.; Aarhus, R.; Walseth, T. F. Calcium mobilization by dual receptors during fertilization of sea urchin eggs. *Science* **1993,** *261*(5119), 352-355.

4. Petersen, O. H.; Michalak, M.; Verkhratsky, A. Calcium signalling: past, present and future. *Cell Calcium* **2005,** *38*(3-4), 161-169.

5. Abraham, T.; Schooling, S. R.; Nieh, M. P.; Kučerka, N.; Beveridge, T. J.; Katsaras, J. Neutron diffraction study of Pseudomonas aeruginosa lipopolysaccharide bilayers. *J.Phys.Chem.B* **2007,** *111*(10), 2477-2483.

6. Binder, H.; Arnold, K.; Ulrich, A. S.; Zschornig, O. Interaction of Zn2+ with phospholipid membranes. *Biophys.Chem.* **2001,** *90*(1), 57-74.

7. Christianson, D. W. Structural biology of zinc. *Adv.Protein.Chem.* **1991,** *42* 281-355.

8. Krezel, A.; Maret, W. The biological inorganic chemistry of zinc ions. *Arch.Biochem.Biophys.* **2016**.

9. Lis, L. J.; Parsegian, V. A.; Rand, R. P. Binding of divalent cations of dipalmitoylphosphatidylcholine bilayers and its effect on bilayer interaction. *Biochemistry* **1981,** *20*(7), 1761-1770.

10. Uhríková, D.; Kučerka, N.; Lengyel, A.; Pullmannová, P.; Teixeira, J.; Murugova, T.; Funari, S. S.; Balgavý, P. Lipid bilayer - DNA interaction mediated by divalent metal cations: SANS and SAXD study. *Journal of Physics: Conference Series* **2012,** *351*(1), 012011.

11. Alsop, R. J.; Maria, S. R.; Rheinstadter, M. C. Swelling of phospholipid membranes by divalent metal ions depends on the location of the ions in the bilayers. *Soft Matter* **2016,** *12*(32), 6737-6748.

12. Petrache, H. I.; Tristram-Nagle, S.; Harries, D.; Kučerka, N.; Nagle, J. F.; Parsegian, V. A. Swelling of phospholipids by monovalent salt. *J.Lipid Res.* **2006,** *47*(2), 302-309.

13. Valley, C. C.; Perlmutter, J. D.; Braun, A. R.; Sachs, J. N. NaCl interactions with phosphatidylcholine bilayers do not alter membrane structure but induce long-range ordering of ions and water. *J.Membr.Biol.* **2011,** *244*(1), 35-42.

14. Rappolt, M.; Pressl, K.; Pabst, G.; Laggner, P. Lalpha-phase separation in phosphatidylcholine-water systems induced by alkali chlorides. *Biochim.Biophys.Acta* **1998,** *1372*(2), 389-393.

15. Pabst, G.; Hodzic, A.; Strancar, J.; Danner, S.; Rappolt, M.; Laggner, P. Rigidification of neutral lipid bilayers in the presence of salts. *Biophys.J.* **2007,** *93*(8), 2688-2696.

16. Uhríková, D.; Kučerka, N.; Teixeira, J.; Gordeliy, V.; Balgavý, P. Structural changes in dipalmitoylphosphatidylcholine bilayer promoted by Ca2+ ions: a small-angle neutron scattering study. *Chem.Phys Lipids* **2008,** *155*(2), 80-89.

17. Brzustowicz, M. R.; Brunger, A. T. X-ray scattering from unilamellar lipid vesicles . *J.Appl.Cryst.* **2005,** *38* 126-131.

18. Harroun, T. A.; Kučerka, N.; Nieh, M. P.; Katsaras, J. Neutron and X-ray scattering for biophysics and biotechnology: examples of self-assembled lipid systems. *Soft Matter* **2009,** *5*(14), 2694-2703.

19. Kučerka, N.; Katsaras, J.; Nagle, J. F. Comparing membrane simulations to scattering experiments: introducing the SIMtoEXP software. *J.Membr.Biol.* **2010,** *235*(1), 43-50.

20. Poger, D.; Caron, B. ; Mark, A. E. Validating lipid force fields against experimental data: Progress, challenges and perspectives. *Biochim.Biophys.Acta* **2016,** *1858*(7 Pt B), 1556-1565.

21. Tristram-Nagle, S. Preparation of oriented, fully hydrated lipid samples for structure determination using X-ray scattering. *Methods Mol.Biol.* **2007,** *400* 63-75.

22. Xia, Y.; Li, M.; Kučerka, N.; Li, S.; Nieh, M. P. In-situ temperature-controllable shear flow device for neutron scattering measurement--an example of aligned bicellar mixtures. *Rev.Sci.Instrum.* **2015,** *86*(2), 025112.

23. Nagle, J. F.; Akabori, K.; Treece, B. W.; Tristram-Nagle, S. Determination of mosaicity in oriented stacks of lipid bilayers. *Soft Matter* **2016,** *12*(6), 1884-1891.

24. Kučerka, N.; Nieh, M. P.; Pencer, J.; Sachs, J. N.; Katsaras, J. What determines the thickness of a biological membrane. *Gen.Physiol Biophys.* **2009,** *28*(2), 117-125.

25. Greenspan, L. Humidity Fixed Points of Binary Saturated Aqueous Solutions. *JOURNAL OF RESEARCH of the National Bureau of Standards - A.Phys ics and Chemistry* **1977,** *81A*(1), 89-96.

26. Liu, Y.; Nagle, J. F. Diffuse scattering provides material parameters and electron density profiles of biomembranes. *Phys.Rev.E* **2004,** *69*(4 Pt 1), 040901.

27. Van Der, S. D.; Lindahl, E.; Hess, B.; Groenhof, G.; Mark, A. E.; Berendsen, H. J. GROMACS: fast, flexible, and free. *J.Comput.Chem.* **2005,** *26*(16), 1701-1718.

28. Castillo, N.; Monticelli, L.; Barnoud, J.; Tieleman, D. P.   Free energy of WALP23 dimer association in DMPC, DPPC, and DOPC bilayers . *Chem.Phys Lipids* **2013,** *169* 95-105.

29. Berger, O.; Edholm, O.; Jahnig, F. Molecular dynamics simulations of a fluid bilayer of dipalmitoylphosphatidylcholine at full hydration, constant pressure, and constant temperature. *Biophys.J.* **1997,** *72*(5), 2002-2013.

30. Allen, W. J.; Lemkul, J. A.; Bevan, D. R. GridMAT-MD: a grid-based membrane analysis tool for use with molecular dynamics. *J.Comput.Chem.* **2009,** *30*(12), 1952-1958.

31. Worcester, D. L.; Franks, N. P. Structural analysis of hydrated egg lecithin and cholesterol bilayers. II. Neutrol diffraction. *J.Mol.Biol.* **1976,** *100*(3), 359-378.

32. Nagle, J. F.; Wilkinson, D. A. Lecithin bilayers. Density measurement and molecular interactions. *Biophys.J.* **1978,** *23*(2), 159-175.

33. Glasser, L.; Jenkins, H. D. Internally consistent ion volumes and their application in volume-based thermodynamics. *Inorg.Chem.* **2008,** *47*(14), 6195-6202.

34. Nagle, J. F.; Wiener, M. C. Relations for lipid bilayers. Connection of electron density profiles to other structural quantities. *Biophys.J.* **1989,** *55*(2), 309-313.

35. Sears, V. F. Neutron scattering lengths and cross sections. *Neutron News* **1992,** *3*(3), 26-37.

36. Yamada, L.; Seto, H. ; Takeda, T.; Nagao, M.; Kawabata, Y.; Inoue, K. SAXS, SANS and NSE Studies on "Unbound State" in DPPC/Water/CaCl2 System. *J.Phys.Soc.Jpn.* **2005,** *74*(10), 2853-2859.

37. Inoko, Y.; Yamaguchi, T.; Furuya, K.; Mitsui, T. Effects of cations on dipalmitoyl phosphatidylcholine/cholesterol/water systems. *Biochim.Biophys.Acta* **1975,** *413*(1), 24-32.

38. Aroti, A.; Leontidis, E.; Maltseva, E.; Brezesinski, G. Effects of Hofmeister Anions on DPPC Langmuir Monolayers at the AirGĺÍWater Interface. *J.Phys.Chem.B* **2004,** *108*(39), 15238-15245.

39. Böckmann, R. A.; Grubmüller, H. Multistep Binding of Divalent Cations to Phospholipid Bilayers: A Molecular Dynamics Study. *Angewandte Chemie International Edition* **2004,** *43*(8), 1021-1024.

40. Bock, C. W.; Markham, G. D.; Katz, A. K.; Glusker, J. P. The arrangement of first- and second-shell water molecules in trivalent aluminum complexes: results from density functional theory and structural crystallography. *Inorg.Chem.* **2003,** *42*(5), 1538-1548.

41. David, F.; Vokhmin, V.; Ionova, G. Water characteristics depend on the ionic environment. Thermodynamics and modelisation of the aquo ions. *Journal of Molecular Liquids* **2001,** *90*(1), 45-62.

42. Sharma, G.; Stevens, C. F. Interactions between two divalent ion binding sites in N-methyl-D-aspartate receptor channels. *Proc.Natl.Acad.Sci.U.S.A* **1996,** *93*(24), 14170-14175.

43. Chaplin, M. Do we underestimate the importance of water in cell biology? *Nat.Rev.Mol.Cell Biol.* **2006,** *7*(11), 861-866.

44. Cauet, E.; Bogatko, S.; Weare, J. H.; Fulton, J. L.; Schenter, G. K.; Bylaska, E. J. Structure and dynamics of the hydration shells of the Zn(2+) ion from ab initio molecular dynamics and combined ab initio and classical molecular dynamics simulations. *J.Chem.Phys* **2010,** *132*(19), 194502.

45. Kruczek, J.; Chiu, S. W.; Jakobsson, E.; Pandit, S. A. Effects of Lithium and Other Monovalent Ions on Palmitoyl Oleoyl Phosphatidylcholine Bilayer. *Langmuir* **2017,** *33*(4), 1105-1115.

46. Gresh, N.; Šponer, J. Complexes of Pentahydrated Zn2+ with Guanine, Adenine, and the Guanine-Cytosine and Adenine-Thymine Base Pairs. Structures and Energies Characterized by Polarizable Molecular Mechanics and ab Initio Calculations. *J.Phys.Chem.B* **1999,** *103*(51), 11415-11427.

47. Remsungnen, T.; Rode, B. M. Molecular dynamics simulation of the hydration of transition metal ions: the role of non-additive effects in the hydration shells of Fe2+ and Fe3+ ions. *Chemical Physics Letters* **2004,** *385*(5-6), 491-497.

Table of Contents Graphic